SLAC-PUB-3118
May 1983
(M)

RESULTS FROM MAC*

George B. Chadwick

for the MAC Collaboration - Colorado, Frascati, Houston, Northeastern, SLAC/Stanford, Utah, Wisconsin Universities

Stanford University, Stanford, California 94305

ABSTRACT

The MAC detector has been exposed at PEP to 40 pb^{-1} luminosity of e^+e^- collisions. The detector is described and recent results of a continuing analysis of hadronic cross section, lepton pair charge asymmetry, Bhabha process, two photon final state and radiative μ pairs are given. New results on "flavor tagging" of hadronic events with an inclusive μ, and some searches for new particles are presented.

INTRODUCTION

The MAC detector (MAgnetic Calorimeter) endeavors to capture all possible observable energies from e^+e^- collision events at PEP, the SLAC storage ring. The large mass needed for this makes the detector an excellent muon identifier, and so the iron of the calorimeter is magnetized to provide a muon momentum measurement. To maximize capture at reasonable cost requires the charged particle tracking chamber to be small. Loss of resolution here is partially compensated for by decreased particle decay probability. The detector thus specializes in the following areas: total hadronic cross section, lepton pair properties, "flavor tagging" with muons, and new particle searches.

The detector has collected an integrated luminosity of ~40 pb^{-1}, most of which data is used in the analyses presented.

* Work supported by the Department of Energy, contract number DE-AC03-76SF00515.

(Invited talk presented at the Europhysics Study Conference on Electroweak Effects at High Energies, Erice, Italy, February 1-10, 1983.)

THE DETECTOR

Figure 1 shows end and side views of the detector. Going out radially from the beam pipe there is first a central drift (CD) chamber of 10 layers in a ~1 m diameter solenoid of 5.7 kG field. Next are six sextants of shower chambers (SC), constructed of lead plates and proportional chamber layers wired into 192 azimuthal cells with layers grouped into 3 sections. An axial coordinate is obtained by current division. Scintillator trigger counters (TC) follow, then comes the central hadron calorimeter (HC) of 2.5 cm steel plates for a total thickness ~1 m, interleaved with proportional chambers wired like the SC, including current division. As noted above, the iron is excited toroidially to ~17 kG by the coils shown. Finally, four layers of drift chamber tubes (MO) are mounted on the iron, which can locate muon tracks exiting the iron and provide a momentum determination.

The endcaps (EC) are made of iron plates, also magnetized, sandwiched with proportional chambers. The segmentation is coarser here than for the central part of the detector, except for a small angle region used for shower detection. The endcaps are followed by six layers of drift tubes (MO) for muon detection: each layer is set at a 60^{o} rotation to the preceding one to allow spatial reconstruction.

The trigger counters (TC) of scintillator, already mentioned, are positioned after the SC, providing a hexagonal "barrel" enclosure, and two end walls of scintillator are set within the EC

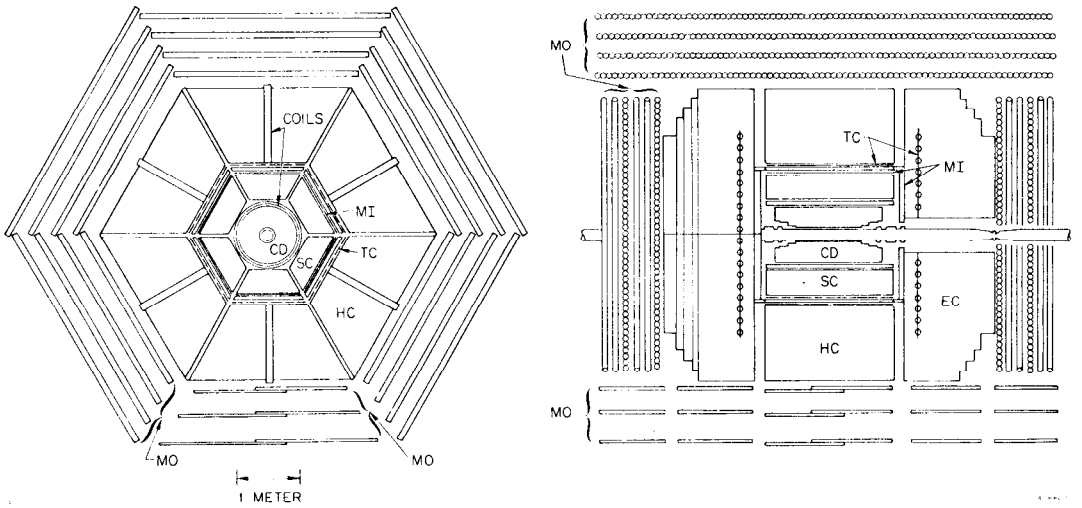

Fig. 1. MAC detector end and side views. Components are: central drift chamber (CD), shower chamber (SC), trigger/timing scintillation counters (TC), central and endcap hadron calorimeters (HC,EC), and inner and outer muon drift chambers (MI,MO).

steel, as shown in Fig. 1. These provide time of flight measurement as well as forming a part of the hardware trigger. The resolution properties of the detector are described in Table I. More details can be found in Ref. 1.

Table I. Resolution of the various sections of the MAC detector.

Section	Resolution	Comments
Central Detector	$\Delta p/p = 0.06 p_\perp$	200μ in space
Shower Chamber	$\Delta E/E = 0.2/\sqrt{E}$	Gaussian part
	$\sigma_\phi = 0.8^o$	segmentation
	$\sigma_\theta = 1.3^o$	current division
Endcap SC	$\Delta E/E = 0.45/\sqrt{E}$	
	$\sigma_\phi = 2^o$	cathode strips
	$\sigma_\theta = 1.5^o$	anode wire groups
Central and Endcap Hadron Calorimeter	$\Delta E/E = 0.87/\sqrt{E}$	
Outer Muon Drift Chambers	$\Delta p/p = 0.3$	multiple scattering limited

HADRONIC TOTAL CROSS SECTION

The hadronic total annihilation cross section is expressed as a ratio R between hadron production and the purely QED production of muon pairs. The latter has a cross section

$$\sigma_0 = \sigma(e^+e^- \to \gamma \to \mu^+\mu^-) = 4\pi\alpha^2/3s \quad .$$

At $\sqrt{s}$ = 29 GeV, our running energy, σ_0 = 0.103 nb.

Experimentally

$$R = \frac{1}{\sigma_0} \cdot \frac{N_{h,corr}}{A} \cdot \frac{1}{\int L\,dt}$$

where $N_{h,corr}$ is the number of purely hadronic events corrected for detector efficiency, background subtraction, and radiative processes. A is the apperture and $\int L\,dt$ is the integrated luminosity.

For hadron production purely by known quark pairs, with no final state interactions, the theoretical expectation for the basic process is

$$R_0 = 3 \sum_f \left(\frac{q_f}{q_e}\right)^2 = \frac{11}{3}$$

where q_e is the electron charge and q_f is the quark charge for flavors f = u,d,s,c,b. A correction for gluon radiation is also postulated,[2] giving

$$R = R_0(1 + \alpha_s/\pi + \ldots) = 1.06\ R_0$$

for $\alpha_s = 0.17$, the most commonly quoted value.[3,4] This implies $R = 3.90$.

Experimentally, the ratio $N_{h,corr}/A$ is determined as a unit by a Monte Carlo procedure in which the computer code of Berends and Kleiss[5] is used to generate quark pairs. This procedure takes into account all radiative processes to order α^3. The quarks are then subjected to hadronic fragmentation using the Lund Monte Carlo procedure.[6] Finally, each event is subjected to a Monte Carlo simulation of the detector response, and the cuts applied to real data are used on the simulation.

The term $\int L\,dt$ is determined in three independent ways: a) by the corrected number of central section Bhabha events (polar angles 55^o-125^o); b) by endcap Bhabhas (15^o-25^o); and c) by a separate luminosity monitor at ~30 mr.

The first data cuts used were based on the energy flow, a vector for each calorimeter cell of the detector, $(E_i, \theta_i\ \phi_i)$. These cuts were:

1. $E_{vis} = \sum |E_i| > 12$ GeV
2. $E_{vis,\perp} = \sum |E_i| \sin\theta_i > 7.5$ GeV
3. Imbalance $I = |\sum \vec{E}_i|/E_{vis} < 0.65$.

In the second set of cuts, at least 3 good CD tracks were required ($\sum |p_i| > 2$ GeV/c, fit to a common vertex). The vertex position $|Z_{vertex}|$ had to be <5 cm, and the total of all tracks >4. With these cuts defining $N_{h,corr}$, the corresponding A is found to be 1.08.

The major corrections applied, and the estimated systematic errors were as follows:

1) virtual $\gamma\gamma \to$ hadrons, 1% ± 0.5%
2) $\tau \to$ 6 prongs, 0.5% ± 0.3%
3) other (pileup etc.), 0.5% ± 0.5% .

The final numbers were $N_{h,corr} = 10{,}870$ events, $\int L\,dt = 24.6\ pb^{-1}$, giving

$$R = 3.97 \pm 0.04 \pm 0.12 \pm 0.12 \ .$$

Here the uncertainties are respectively statistical, experimental systematic, and theoretical uncertainty in higher order (α^4) corrections. The overall uncertainty is 4.2%. This result compares favorably with previously reported values.[7]

The agreement with simple QCD is striking; the 6% α_s correction seems beautifully confirmed. It is clear that the production of a

charge 2/3 top quark pair is ruled out, and the presence of a charge 1/3 quark is very unlikely. At this energy there is no detectable affect on R from the weak interactions.

MUON PAIR PRODUCTION CHARGE ASYMMETRY

In the standard model, muon pairs are expected to show a detectable asymmetry in the angular distribution of μ^+ with respect to the initial e^+ beam direction, owing to interference between annihilation through γ and through Z^o intermediate states:

$$\frac{d\sigma}{d\cos\theta} = \frac{\pi\alpha^2}{2s}\left[R_{\mu\mu}(1+\cos^2\theta) + B\cos\theta\right]$$

$$R_{\mu\mu} = 1 + 2g_V^2\chi \approx 1 \qquad \text{(to order } \alpha G\text{)}$$

$$B = 4g_A^2\chi$$

$$\chi = \frac{G_F}{2\sqrt{2}\,\pi\alpha}\,\frac{s}{s/M_Z^2 - 1}$$

where the symbols have their well known meanings. The charge asymmetry

$$A_{\mu\mu} = \frac{N_F - N_B}{N_F + N_B} = \frac{3B}{8R_{\mu\mu}}$$

is predicted this way to be -6.3% at $\sqrt{s}$ = 29 GeV. Using a recent modification of the standard Monte Carlo procedure which includes radiation on the Z^o diagrams,[8] the expected asymmetry becomes -6.0%.

Experimentally, detector fields were reversed periodically. The data was selected as follows:

1. Two CD track found, vertex constrained, and associated with minimum ionizing tracks in shower and hadron calorimeters and/or muon track in the OD system.
2. CD momenta satisfy $|p_1| + |p_2| > 8$ GeV/c.
3. $|z_{vertex}| < 5$ cm, $|x_v| < 0.4$ cm, $|y_v| < 0.2$ cm.
4. Scintillator time difference $-10 < \Delta t < 4$ nsec.
5. Acollinearity angle $<10^o$.
6. Opposite signs of momenta (CD or OD).

We have only recently incorporated the OD muon detectors into the analysis. This has helped to reduce charge sign ambiguities and identify some feed-in of forward Bhabha events, which are highly asymmetric. Background estimates are:

1. Cosmic rays, < 0.5%
2. $ee\mu\mu$, ~ 1.8%
3. Bhabhas , < 0.3%
4. $\tau\tau$ events , 2.5%

The final sample had 3067 events, with 130 attributed to background. Integrated luminosity was 39.9 pb^{-1}. For this data the observed asymmetry was corrected for an asymmetry from QED processes[8] of +2.8%, to give

$$A_{\mu\mu} = - 0.076 \pm 0.018 \pm 0.003 \quad .$$

For M_Z = 90 GeV, this implies via the standard model

$$g_A^e \, g_A^\mu = 0.31 \pm 0.08 \quad .$$

If the expected value of 0.25 is used as input, the asymmetry implies

$$M_Z > 40 \text{ GeV}$$

at 90% confidence level.

When all detector efficiencies are included, the normalization of the reaction gives

$$R_{\mu\mu} = 0.99 \pm 0.02 \pm 0.05 \quad .$$

This result implies

$$g_V^e \, g_V^\mu = 0.03 \pm 0.16 \quad .$$

Both results are in excellent agreement with measurements from other detectors (see paper of A. Böhm, this conference).

The analysis of τ pair processes for charge asymmetry remains as reported at the Paris Conference.[4]

BHABHA SCATTERING

The elastic scattering reaction has its charge asymmetry overwhelmed by the intensity of the t-channel process. However the angular distribution is modified by electroweak effects, even if $\sin^2\theta_W = 0.25$. This process is so prolific that very small errors are possible, and an understanding of the data provides an excellent assurance that one understands the detector response.

Events were selected with two vertex constrained CD tracks, collinear to 10^o, and having a total energy in the shower counters of over 0.5 $E_{c.m.}$. Corrections were made for tracking efficiencies, energy cut efficiencies, and radiative corrections with the standard Monte Carlo techniques. In these events no external charge

identification is available, and so the small CD double sign reversal ambiguity puts enough forward high cross section events into the backward hemisphere to spoil the beauty of the distribution. Fortunately, little actual sensitivity is lost in the fit to a folded distribution.

In Fig. 2, the angular distribution is shown as a ratio to the pure QED prediction. The solid line shows the best fit for a variation of $\sin^2\theta_W$. The broken line shows the charge for a 95% confidence level variation, in either direction. The result is

$$\sin^2\theta_W = 0.24 \pm 0.08 \quad .$$

The statistical level of data from this reaction has reached a point at which a significant test of "preon" models of composite leptons can be made. Details may be found elsewhere,[9] but briefly, composite structure would imply constituent exchange, which would induce an effective contact interaction of the form

$$\frac{g^2}{2\Lambda^2}\,\eta_{ij}\,\bar{\psi}_i\,\gamma_\mu\,\psi_i\,\bar{\psi}_j\,\gamma_\mu\,\psi_j$$

where i,j are over left and right handed spinors. $g^2/4\pi$ is taken equal to unity (making Λ a "mass scale" rather than an actual mass) and η's are zero or ± 1. Interference with the normal exchange process would produce a deviation from QED of a quite marked character, for masses in the usual range of testing.

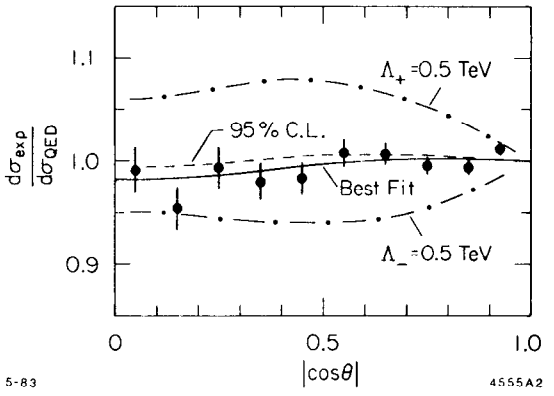

Fig. 2. Angular distribution of the reaction $e^+e^- \to e^+e^-$ compared with QED. BEST FIT is from varying $\sin^2\theta_W$ and 95% C.L. is from such a variation. The dot-dashed lines are meant to show the sensitivity of the data to preon mass.

The dot-dash lines of Fig. 2 show a prediction for $\Lambda_{RR} = 0.5$ TeV, which would produce a wildly unacceptable fit. At the 95% confidence level, actual fits produce the limits:

$$\eta_{LL} = 1, \quad \eta_{RR} = \eta_{RL} = 0 : \Lambda_{LL} > 1.2 \text{ TeV}$$
$$\eta_{RR} = \eta_{LL} = \eta_{RL} = 1 : \Lambda_{VV} > 2.5 \text{ TeV}$$
$$\eta_{RR} = \eta_{LL} = 1, \ \eta_{RL} = -1 : \Lambda_{AA} > 1.3 \text{ TeV}$$

where V and A stand for vector and axial vector coupling combinations.

TWO PHOTON FINAL STATE

The process

$$e^+e^- \to \gamma\gamma$$

shows no effects from weak interactions, and hence provides the cleanest test of QED theory. When the experimental angular distribution is compared with QED, deviation from agreement are parameterized as the mass of an excited or "ortho" electron which can be exchanged. The cross section becomes

$$d\sigma/d\Omega = (d\sigma/d\Omega)_{QED} \ (1 + s^2 \sin^2\theta/2\Lambda^4)$$

where Λ is the e^* mass.

We have found our data to be consistent with QED. At the 95% confidence level

$$\Lambda = M_{e^*} < 55 \text{ GeV} \quad .$$

RADIATIVE MUON PAIRS

The interest in the reactions

$$e^+e^- \to \mu\mu^* \to \mu\mu\gamma \qquad (1)$$

is twofold. First, it provides a search for an "orthomuon," i.e. an excited state. Secondly, it provides an excellent test of our understanding of radiative corrections. Thus we win either way.

Process (1) is described by[10]

$$\frac{d\sigma}{d\Omega} = \lambda^2 \alpha^2 \ \frac{(s-M)^2}{s^3} \left[(s+M^2) - (s-M^2) \ \cos^2\theta\right]$$

which is quite distinguishable from the usual Bremsstrahlung. Here λ is a factor modifying the usual coupling of pairs.

If such a state as μ^* exists, we would also expect to see the process

$$e^+e^- \to \mu^*\mu^* \to \mu\mu\gamma\gamma \qquad (2)$$

with an equally distinctive distribution

$$\frac{d\sigma}{d\Omega} = \frac{\alpha^2}{4s} |F(s)|^2 \beta\left[1 + \cos^2\theta + (1 - \beta^2) \sin^2\theta\right] .$$

Therefore we study both final states.

The $\mu\mu\gamma$ event sample was selected by the following criteria:

1. Two tracks, satisfying muon criteria, with collinearity $> 10^o$.
2. $E_\gamma > 1$ GeV.
3. Acceptable 4-constraint kinematic fit.

The $\mu\mu\gamma\gamma$ selection used the above, plus an extra requirement of $>10^o$ between any tracks or showers.

The invariant $\mu\gamma$ mass for reaction (1) is shown in Fig. 3(a). Superimposed is the QED prediction (Berends-Kleiss[5]), in excellent agreement. In Fig. 3(b) the angular distribution is shown, with the QED prediction. A strong charge asymmetry, well explained, is evident, of around -20%. Its source is interference between initial and final state real radiation. At large angles and energies the two sources become comparable, but have different intermediate state C parities.

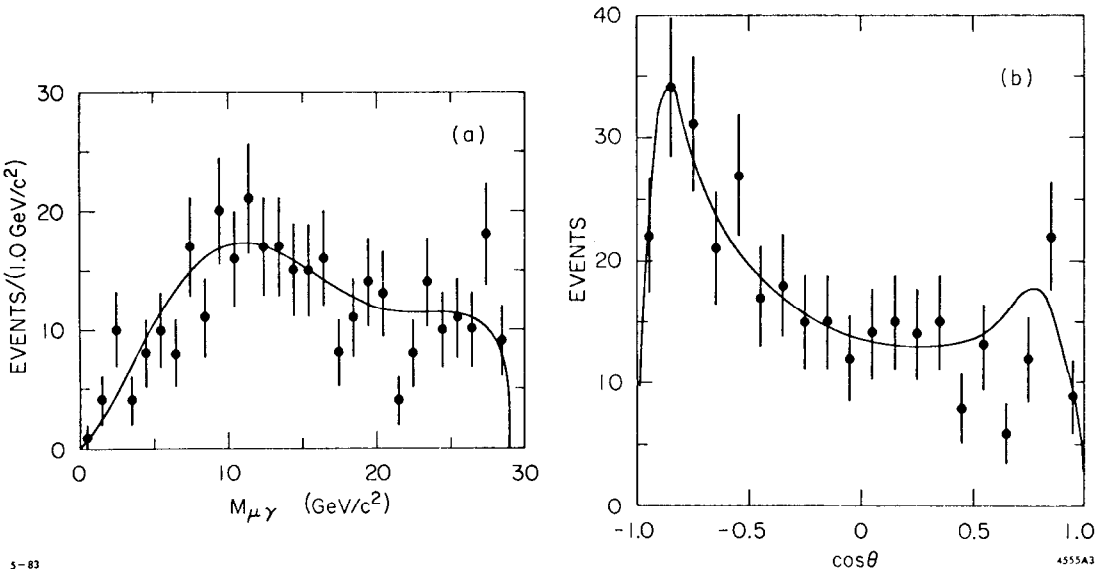

Fig. 3. (a) Invariant mass of $\mu\gamma$ system in the reaction $e^+e^- \to \mu^+\mu^-\gamma$. The solid curve is the absolute QED prediction; (b) angular distribution of the same reaction, along with the QED prediction, both showing a strong charge asymmetry.

In Fig. 4(a) we show a scatter plot for reaction (2) $\mu\gamma$ masses. If a $\mu^*\mu^*$ pair was being made, the area enclosed by broken lines would have an enhanced population, which is not found. Figure 4(b) shows the 95% confidence level mass limits assigned as a function of $M_{\mu\gamma}$ and effective couplings assumed.

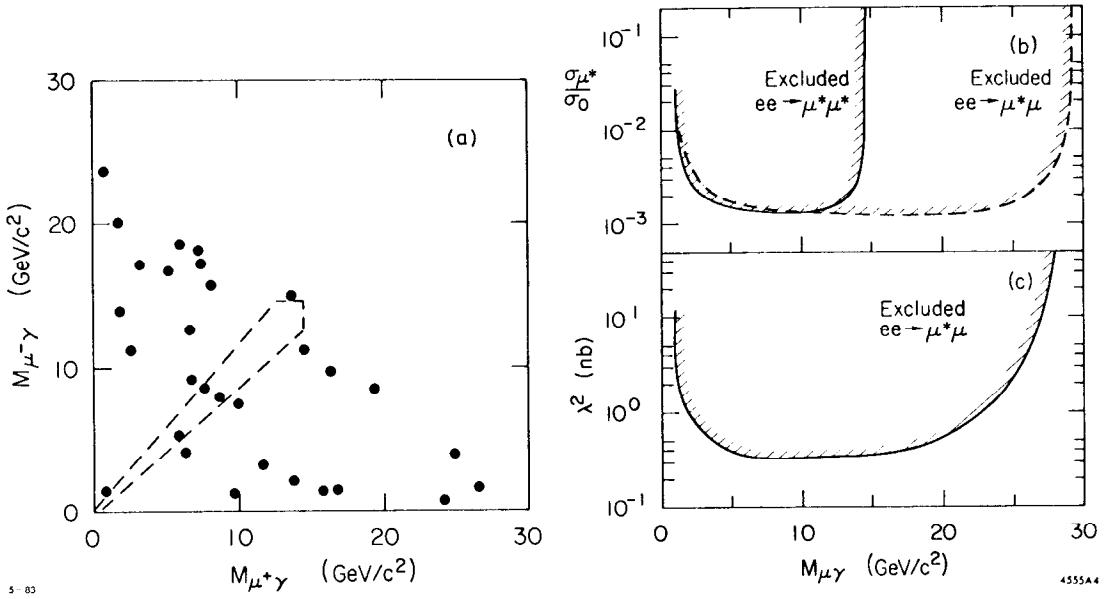

Fig. 4. (a) Scatter plot of invariant $\mu\gamma$ masses in the reaction $e^+e^- \to \mu^+\mu^-\gamma\gamma$. Each event appears twice. The broken line indicates the search area for an excess of events due to excited muon production; (b) mass limits (95% confidence level) for the excited muon state corresponding to assumed parameters of the production process given in the text.

INCLUSIVE MUON FLAVOR TAGGING

With the MAC detector surrounded by drift tubes, it is possible to identify muons in hadronic events, measure their momentum, and deduce their initial angles. A large momentum transverse to the jet axis carried by the muon is indicative of a massive quark semi-leptonic decay. The main background is from muonic decay of π or K mesons and "punch-through" of hadrons. Our estimates of these backgrounds in the selected sample are 20% and 10% respectively.

A total of 240 events were selected from a 27 pb^{-1} data sample. The muon momentum transverse to the event thrust axis, $p_\perp$, is shown in Fig. 5(a). Superimposed upon the histogram are the expected distributions from b and c quark decays and from background. This decomposition was arrived at by first deducing a quark fragmentation spectrum,[11] then fitting the data assuming a semi-muonic decay fraction. The Ali[12] Monte Carlo procedure was used.

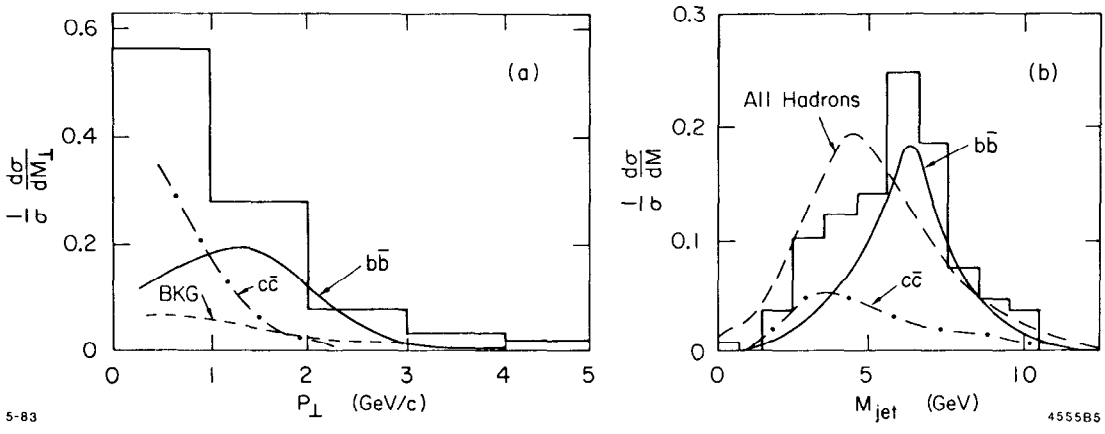

Fig. 5. (a) Muon momenta perpendicular to the thrust axis in hadronic annihilation events with an identified "inclusive muon." Curves indicate the contributions from $b\bar{b}$ (solid), $c\bar{c}$ (broken) and background (dot-dash) production processes as obtained in an overall fit; (b) jet mass, defined in the text, for above events with $p_\perp$ > 1 GeV/c. Fit determined contributions are again indicated.

For the jet opposite the one with the muon, a "jet mass" is calculated:

$$M_{jet} = E_{beam}\sqrt{1 - T_{1/2}^2}$$

where $T_{1/2}$ is the thrust of particles in the jet hemisphere. Figure 5(b) shows the normalized distribution for $p_\perp$ > 1 GeV/c, the b quark selection cut. Superimposed is the jet mass found for all hadronic events (broken line) which peaks noticeably lower. We note parenthetically that for $p_\perp$ < 1 GeV/c, the jet mass agrees with the "all hadron" curve. The solid lines show the deduced $b\bar{b}$ and $c\bar{c}$ contributions. A cut for M_{jet} > 5 GeV further enhances the b signal.

The charge asymmetry for quark pairs is expected to be larger than for μ pairs, i.e.

$$A_{ff} = \frac{3\chi}{2Q_f}\, g_A^e\, g_A^f$$

because for $b\bar{b}$, $Q_f = 1/3$. We naively expect $A_{bb} \approx -19\%$. Unfortunately, with the above cuts, only 64 events remain, and we find

$$A_{bb} = 0.06 \pm 0.13$$

which is not a significant test. Further data and deeper analysis will be needed to use this promising technique.

SUMMARY

MAC has now produced results which in each test confirm the validity of the Standard Electroweak Model. Its future now lies in the search for phenomena outside that model.

REFERENCES

1. W. T. Ford, SLAC-PUB-2894 (1982).
2. M. Dine and J. Sapirstein, Phys. Rev. Lett. 43:668 (1979).
3. D. P. Barber et al., Phys. Lett. 89B:139 (1979); R. Brandelik et al., Phys. Lett. 94B:459 (1980); D. Schlatter et al., Phys. Rev. Lett. 49:521 (1982).
4. D. M. Ritson, Contribution to XXI International Conference on High Energy Physics, Paris, 1982 (SLAC-PUB-2986, Oct. 1982).
5. F. A. Berends and R. Kleiss, Nucl. Phys. B177:237 (1981); Nucl. Phys. B178:141 (1981).
6. T. Sjostrand, University of Lund Report LUND LU TP 82-3, 82-7 (1982, unpublished).
7. See e.g. K. H. Mess and B. H. Wiik, DESY 82-011 (1982).
8. F. A. Berends, R. Kleiss and S. Jadach, Nucl. Phys. B202:63 (1982).
9. E. J. Eichten, K. D. Lane and M. E. Peskin, FERMILAB-PUB-83/15-THY (1982).
10. F. E. Low, Phys. Rev. Lett. 14:238 (1965).
11. W. T. Ford et al., to be published.
12. A. Ali et al., Phys. Lett. 93B:155 (1980).